International Journal of Bifurcation and Chaos, Vol. 23, No. 8 (2013) 1350132 (12 pages)

DOI: 10.1142/S0218127413501320

# STOCHASTIC AND COHERENCE RESONANCES IN A MODIFIED CHUA'S CIRCUIT SYSTEM WITH MULTI-SCROLL ORBITS

S. ARATHI* and S. RAJASEKAR†
*School of Physics, Bharathidasan University, Tiruchirapalli 620 024, Tamilnadu, India*
**arathisreekumari@gmail.com*
†*rajasekar@cnld.bdu.ac.in*
†*srj.bdu@gmail.com*

J. KURTHS
*Potsdam Institute for Climate Impact Research, P. O. Box 601203, Potsdam 14412, Germany*
*kurths@pik-potsdam.de*

Received October 8, 2012; Revised February 27, 2013

We numerically investigate the role of the number of equilibrium points ($N$) on characteristic features of stochastic and coherence resonances in a modified Chua's circuit model equation capable of generating multi-scroll orbits. Both types of resonances are found for $1 < N \leq 20$. Almost periodic switching between the scroll orbits is observed at resonance. The values of the signal-to-noise ratio (used to quantify stochastic resonance), the autocorrelation function and the ratio of the dominant peak and its relative width in the power spectrum of the output signal (used to characterize coherence resonance) at resonance increase with $N$, reaching a maximum at $N = 6$ and then decrease. The mean residence time of a scroll orbit at resonance decreases rapidly with $N$. We show that both resonances in the multi-scroll orbits can be useful for weak signal detection.

*Keywords*: Modified Chua's circuit equation; stochastic resonance; coherence resonance; signal detection.

## 1. Introduction

Stochastic resonance is one of the most remarkable phenomena in nonlinear dynamics. In a typical bistable system driven by a weak periodic signal of frequency $\omega$, the output signal-to-noise ratio (SNR) displays nonmonotonic behavior as a function of the input noise intensity. This noise-induced phenomenon called stochastic resonance (SR) has been studied theoretically, numerically and experimentally in a variety of physical, biological and engineering systems [Jung, 1993; Gammaitoni *et al.*, 1998; McDonnell *et al.*, 2008] over the past three decades. Its occurrence is analyzed in overdamped and underdamped bistable systems, monostable systems driven by multiplicative noise (to induce bistability) and in monostable systems with coexisting attractors. Another fundamental resonance-like behavior is observed in the absence of a weak periodic input signal and is termed as coherence resonance (CR) [Pikovsky & Kurths, 1997]. CR was first observed in FitzHugh–Nagumo equations by Pikovsky and Kurths [Pikovsky & Kurths, 1997]. When the noise is replaced by a high-frequency periodic force, the nonlinear systems exhibit resonance behavior and is called vibrational resonance [Landa & McClintock, 2000].

It is important to investigate the features of various dynamics in multi-stable systems or in oscillators with multi-well potentials. This is because there are many nonlinear systems with multi-stable states and moreover such studies help us to know how multi-stable states affect resonance dynamics and explore their role on the characteristics of the resonance. In this connection very recently, the occurrence of vibrational resonance has been analyzed in pendulum systems with a periodic potential [Rajasekar *et al.*, 2011]. In a damped and bi-harmonically driven pendulum when the amplitude of the high-frequency force is varied the amplitude of oscillation at the low-frequency of the force, exhibited a series of resonance approaching a nonzero limiting value. Vibrational ratchet motion is studied in certain systems with spatially periodic potentials driven by a periodic force and a noise [Borromeo & Marchesoni, 2006]. In the pendulum system driven by a high-frequency periodic force and noise, applying vibrational mechanics scheme, it has been shown that mobility and diffusion coefficient are highly sensitive to mass even for large damping [Borromeo & Marchesoni, 2007].

Very little work is done on SR in periodic potential systems. It has been shown that [Kim & Sung, 1998] the resonant behavior exhibited in a pendulum system is not SR associated with the hopping between the wells. The observed resonance is a noise-enhanced phenomenon due to the intra-well motion. In the case of large damping and weak periodic force, the distribution of the escape times displayed a series of SR-like peaks with noise intensity [Kallunki *et al.*, 1999]. Such a characteristic property is not observed with diffusion coefficient. Nicolis [2010] investigated SR in a potential with an arbitrary number of minima and maxima. Employing the linear response theory, the number of minima and maxima giving maximum response is obtained. The occurrence of SR is studied in a pendulum system with the driving frequency close to the natural frequency using the input energy and hysteresis loop area as its characteristic measures [Saikia *et al.*, 2011]. In the spatially periodic potentials like the pendulum system, there are infinite number of minima (which are stable equilibria). In the field of nonlinear electronic circuits, there is a class of circuits capable of producing multi-equilibrium points and multi-scroll attractors. Such circuits can be easily realized. For example, the famous Chua's circuit has been modified to display multi-scroll orbits by adding a desired number of breakpoints. The generation of multi-scroll attractors is realized in a variety of electronic circuits including the modified Brockett's system [Aziz-Alaoui, 1999], circuit with a sign function [Yalcin *et al.*, 2001] or a hyperbolic tangent function [Ozoguz *et al.*, 2002] or a saw-tooth function [Yu *et al.*, 2007], second-order hysteresis system [Han *et al.*, 2003] and jerk circuit [Yu *et al.*, 2005]. Systematic approaches for generating $n$-scroll attractors [Zhong *et al.*, 2002; Lu & Chen, 2006; Campos-Canton *et al.*, 2010] are reported. The study of such circuits explores the influence of multi-equilibrium states on the dynamics exhibited by them.

Motivated by the above considerations, in the present work we wish to investigate the response of a modified Chua's circuit equation with $N$ equilibrium points and with a saw-tooth wave function nonlinearity driven by (i) a weak periodic force and noise, (ii) noise only. That is, especially we are interested in (i) SR and (ii) CR. So far, these two phenomena have not been analyzed in multi-scroll systems. The purpose of our investigation is to explore the role of multiple states on the characteristic features of both SR and CR in the modified Chua's circuit equation and the applicability of these two resonances on weak signal detection. The reason for our interest in Chua's circuit with multiple equilibrium points is multi-fold. This circuit can be used in place of spatially periodic systems like the pendulum system. Multi-scroll attractors have a wide range of theoretical and real world applications. For example, a secure digital communication using a digitized keying method [Tang *et al.*, 2001] is reported. A random bit generator based on a double-scroll chaotic attractor is proposed [Yalcin *et al.*, 2004a, 2004b]. A simple proportional and differential controller to control the $n$-scroll dynamics of Chua's circuit to a stable equilibrium point or to a stable periodic orbit is presented [Boukabou *et al.*, 2009].

For the modified Chua's circuit system with the number of equilibrium points $N$ ranging from 2 to 20, for each fixed value of $N$, the quantity SNR is found to be maximum at an optimum noise intensity ($D_{\mathrm{MAX}}$). $D_{\mathrm{MAX}}$ increases with $N$, while the maximum value of SNR at $D_{\mathrm{MAX}}$ (denoted as $\mathrm{SNR}_{\mathrm{MAX}}$) increases with $N$, becomes a maximum at $N = 6$ and then decreases. For each fixed value of $N$ (2 to 20) at resonance almost

periodic switching between scroll orbits occur. The mean residence time $T_{MR}$ on a scroll orbit at resonance ($D = D_{MAX}$) decreases with $N$. We found $T_{MR}(D_{MAX}) = T/[2(N-1)]$ where $T = 2\pi/\omega$ and $\omega$ is the frequency of the input periodic signal. Because the nonlinearity in the circuit is a symmetric saw-tooth function, $T_{MR}$ on each scroll is the same. We explore the utility of SR in a multi-scroll system in detecting an additional dc or ac signal. Addition of a dc signal creates an asymmetry in the saw-tooth function in the circuit. Consequently, $T_{MR}$ on a particular scroll orbit is different from the other scroll orbits. The difference in the mean residence times, $\Delta T_{MR}$, varies linearly with the increase in the dc signal and this characteristic property can be used as a measure of the presence of a weak dc signal. On the other hand, the presence of an ac signal in the input can be detected from the variation of SNR at the optimum noise intensity, since SNR varies linearly with the amplitude and the frequency of the applied ac signal.

The system is found to show CR in the absence of input periodic signal but in the presence of noise. The power spectrum of the output signal displays a dominant peak at a particular frequency. The autocorrelation function and the ratio of the height of the dominant peak and its relative width in the power spectrum vary with the noise intensity in a fashion similar to SNR in the case of SR. Both quantities become maximum at the same value of the noise intensity. In CR also, the response is maximum for $N = 6$. Similar to SR, at CR almost periodic switching between the coexisting states occurs for $2 < N < 20$. The mean residence time $T_{MR}$ at $D = D_{MAX}$ decreases with $N$.

The paper is organized as follows. In Sec. 2 first we introduce the modified Chua's circuit model equation capable of generating $N$ scroll attractors. We analyze the role of the number of equilibrium states of the circuit model equation on the characteristics of SR. Section 3 is devoted for weak signal detection through SR using the modified Chua's circuit model equation. In Sec. 4 we discuss the effect of the number of equilibrium states on CR. Section 5 contains concluding remarks.

## 2. Stochastic Resonance

The dimensionless form of the modified Chua's circuit model equation [Yu *et al.*, 2007] proposed for generating multi-scroll attractors is given by

$$\dot{x} = \alpha y - \alpha F(x), \tag{1a}$$

$$\dot{y} = x - y + z, \tag{1b}$$

$$\dot{z} = -\beta y + f\sin\omega t + \eta(t), \tag{1c}$$

where

$$\begin{aligned} F(x) &= F_1(x) \\ &= \xi x + \xi A\,\mathrm{sgn}(x) \\ &\quad - \xi A\sum_{j=0}^{n-1}[\mathrm{sgn}(x+2jA) + \mathrm{sgn}(x-2jA)] \end{aligned} \tag{2}$$

or

$$\begin{aligned} F(x) &= F_2(x) \\ &= \xi x - \xi A\sum_{j=0}^{n-1}[\mathrm{sgn}(x+(2j+1)A) \\ &\quad + \mathrm{sgn}(x-(2j+1)A)], \end{aligned} \tag{3}$$

$\alpha$, $\beta$, $\xi$, $A > 0$, $n \geq 1$ and $\mathrm{sgn}(x) = -1, 0, 1$ for $x < 0$, $x = 0$ and $x > 0$ respectively.

$F(x)$ given by Eqs. (2) or (3) is a saw-tooth function with amplitude $2A\xi$ and period $2A$. Figures 1(a) and 1(b) depict the forms of $F_1(x)$ and $F_2(x)$ respectively for $n = 2$, $\xi = 0.25$ and $A = 0.5$. The piecewise-linear functions $F_1(x)$ and $F_2(x)$ have multiple breakpoints. The number of breakpoints depends on the value of $n$ in Eqs. (2) and (3). The breakpoints are given by

$$x_{bp} = \begin{cases} \pm(m-1), & \text{for } F_1(x) \\ \pm\left(m-\dfrac{1}{2}\right), & \text{for } F_2(x), \end{cases} \tag{4}$$

where $m = 1, 2, \ldots, n$. The equilibrium points about which scroll orbits occur are given by

$$(x_e, y_e, z_e) = \begin{cases} [\pm(2m-1)A, 0, \mp(2m-1)A], \\ \qquad\qquad \text{for } F_1(x) \\ (0,0,0), (\pm 2mA, 0, \mp 2mA), \\ \qquad\qquad \text{for } F_2(x), \end{cases} \tag{5}$$

where $m = 1, 2, \ldots, n$. The system (1) in the absence of external forces with $F_1(x)$ possesses $N = 2n$ equilibrium points, while with $F_2(x)$, the system admits $N = 2n+1$ equilibrium points. To realize the

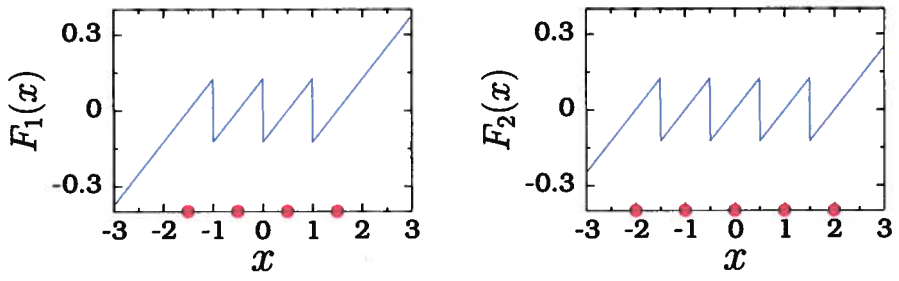


Fig. 1. The graph of (a) $F_1(x)$, (b) $F_2(x)$ given by Eqs. (2) and (3) respectively with $n = 2$, $\xi = 0.25$ and $A_1 = 0.5$. The equilibrium points about which scroll orbits occur are indicated by solid circles. (a) and (b) $n = 2$.

system (1) with an even respectively odd number of equilibrium points, we use the functions $F_1(x)$ and $F_2(x)$ respectively as $F(x)$.

We fix the values of the parameters in Eq. (1) as $\alpha = 6$, $\beta = 14$, $A = 0.5$, $\xi = 0.25$ and $f = 0.07$ so that the noise free system ($\eta(t) = 0$) possesses $N$ coexisting period-$T(= 2\pi/\omega)$ orbits. About each equilibrium point there is one periodic orbit. Each orbit is confined between two consecutive breakpoints. Between two consecutive equilibrium points there is a finite height barrier located at the breakpoints. There is no cross-barrier motion for the above chosen values of the parameters. A barrier crossing can be induced by an additive noise leading to SR. We choose $\eta(t)$ as Gaussian white noise with zero mean and correlation $\langle \eta(t)\eta(s)\rangle = D\delta(t-s)$ where $D$ is the noise intensity. In the numerical analysis, Eq. (1) is integrated with the time step $\Delta t = (2\pi/\omega)/2000$. Starting from an initial condition $(x(0), y(0), z(0))$ near the origin without noise term, Eq. (1) is integrated to get the solution $(x(\Delta t), y(\Delta t), z(\Delta t))$. Noise is then added to the variable $z$ as $z(\Delta t) \to z(\Delta t) + \sqrt{D\Delta t}\,\eta(t)$ where $\eta(t)$ represents Gaussian random numbers with zero mean. In this way noise is added to the state variable in each integration step. We analyze the effect of the number of equilibrium states on the various characteristics of SR.

One of the characteristic measures of SR is SNR given by

$$\text{SNR} = 10\log_{10}\left(\frac{S}{N_s}\right)\text{dB}, \tag{6}$$

where $S$ and $N_s$ are the amplitudes of the signal and the background noise respectively computed from the power spectrum at the frequency $\omega$ of the input signal $f\sin\omega t$. Figure 2 presents the SNR profile for $N \in [2, 20]$. In this figure, we note that for each fixed value of $N$, as the noise intensity $D$ increases from a small value, SNR increases, reaches a maximum value at an optimum noise intensity denoted as $D_{\text{MAX}}$ and then decreases. This is a typical signature of SR phenomenon.

Figure 3 shows typical time-series plots for a few fixed values of $D$ with $F(x) = F_1(x)$ and $n = 1$ ($N = 2$). For small values of $D$ the motion is confined around each of the two equilibrium states as in Fig. 3(a). The two orbits in this figure are obtained for two different initial conditions. The system exhibits a behavior similar to that of the noise free case but in a slightly perturbed form due to the applied noise. As $D$ increases, at $D = D_c$ onset of a cross-barrier behavior occurs. For $D \geq D_c$ the trajectory jumps randomly from one side of the barrier (or the breakpoint) to the other etc. In Fig. 3(b) for $D = 0.04$ the state variable $x$ switches irregularly but occasionally between positive and negative values, that is, between the two sides of the barrier. In a symmetric bistable oscillator with a double-well potential this type of motion

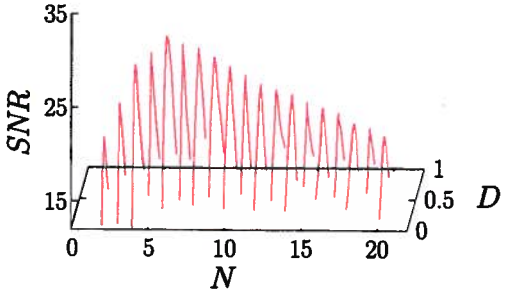


Fig. 2. Variation of signal-to-noise ratio (SNR) as a function of the noise intensity $D$ for the modified Chua's circuit model equation for $N = 2, 3, \ldots, 20$. For $N = 2, 4, \ldots, 20$ the function $F(x)$ in Eq. (1) is chosen as $F_1(x)$ with $n = 1, 2, \ldots, 10$ respectively and for $N = 3, 5, \ldots, 19$ $F(x) = F_2(x)$ with $n = 1, 2, \ldots, 9$, respectively.

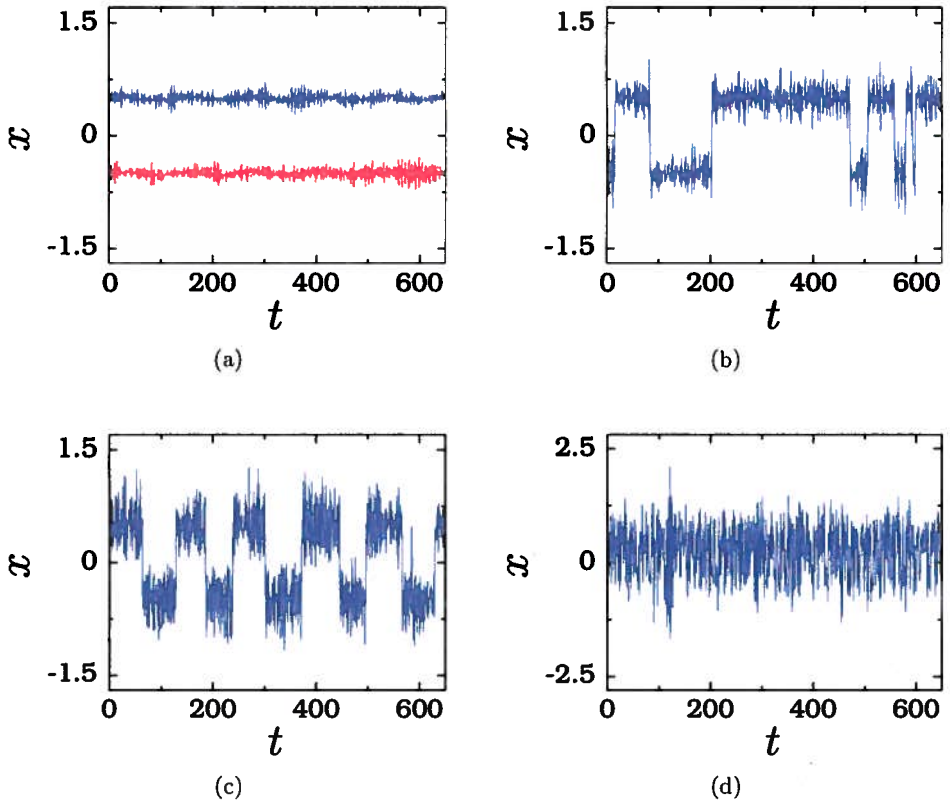


Fig. 3. $x$ versus $t$ of Eq. (1) with two equilibrium points ($N = 2$) for four values of noise intensity $D$. $F(x)$ is chosen as $F_1(x)$ with $n = 1$ so that $N = 2n = 2$. The values of the other parameters are $\alpha = 6$, $\beta = 14$, $A = 0.5$, $\xi = 0.25$, $\omega = 0.05$ and $f = 0.07$. (a) $N = 2$, $D = 0.004$, (b) $N = 2$, $D = 0.04$, (c) $N = 2$, $D_{\mathrm{MAX}} = 0.14$ and (d) $N = 2$, $D = 0.4$.

corresponds to a cross-well orbit and the depth of the well and the local maximum of the potential correspond to the barrier height and the breakpoint respectively in the function $F(x)$. The switching is not periodic for small values of $D$. As the value of $D$ increases further, the switching between the coexisting states increases. At $D = 0.14$ [Fig. 3(c)] almost periodic switching is seen. SNR is maximum at this value of $D$. For sufficiently large values of $D$, the motion is dominated by the noise. In this case the intermittent dynamics disappears and the trajectory jumps erratically between both sides of the barrier. This is shown in Fig. 3(d) for $D = 0.4$.

Figures 4(a) and 4(b) depict the effect of $N$ on $D_{\mathrm{MAX}}$ and $\mathrm{SNR}_{\mathrm{MAX}}$ respectively. $D_{\mathrm{MAX}}$ increases monotonically with $N$ and its variation is a non-linear function of $N$. Though the barrier height remains same at all the breakpoints and same for

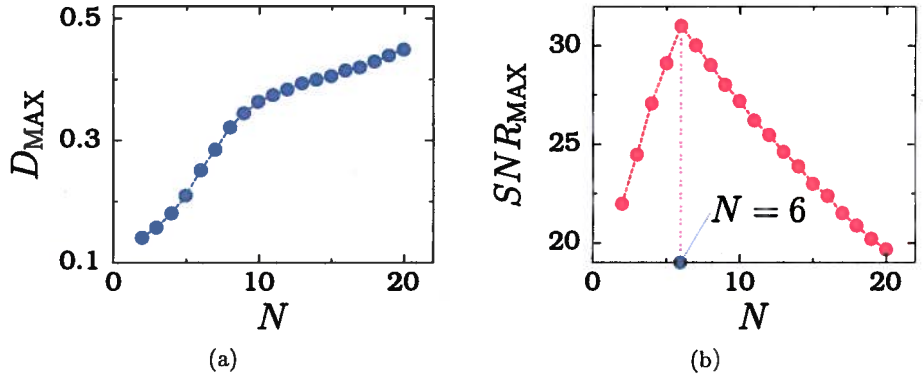


Fig. 4. Variation of (a) $D_{\mathrm{MAX}}$ and (b) $\mathrm{SNR}_{\mathrm{MAX}}$ with the number of equilibrium points $N$.

all values of $N \geq 2$, the value of $D_{\mathrm{MAX}}$ at which resonance occurs depends on $N$. Even though $D_{\mathrm{MAX}}$ increases with $N$, the $\mathrm{SNR}_{\mathrm{MAX}}$ neither increases nor decreases monotonically with $N$ as seen in Fig. 4(b). Interestingly, $\mathrm{SNR}_{\mathrm{MAX}}$ increases with $N$, becomes maximum for $N = 6$ and then decreases. This implies that along with the optimum noise intensity an optimum number of equilibrium points can be used to enhance the SR phenomenon. In this connection we wish to point out that for a pendulum system with $N$ coexisting states, Nicolis [2010] theoretically predicted that there exists an optimal number of coexisting states for which the response of the system at resonance is maximized.

Figure 5 presents the almost periodic switching between the coexisting states at $D = D_{\mathrm{MAX}}$ for $N = 2$, 4 and 6. In this figure, corresponding to the two coexisting states ($N = 2$) the trajectory switches almost periodically between the states. For the case of four and six coexisting states ($N = 4$ and 6 respectively) as shown in Figs. 5(b) and 5(c) respectively the trajectory visits the states one by one say, left most state to the right most state, reverses the direction of visit and so on. We can clearly notice that the time spent about an equilibrium point varies with $N$. When the system (1) has $N$ equilibrium points, then there are $(N-1)$ breakpoints in the function $F(x)$. Suppose we denote the left most breakpoint as $x_{\mathrm{bp}}^{(1)}$, the next breakpoint as $x_{\mathrm{bp}}^{(2)}$ and so on. Let us call the region $x < x_{\mathrm{bp}}^{(1)}$ as $R_1$, $x_{\mathrm{bp}}^{(1)} < x < x_{\mathrm{bp}}^{(2)}$ as $R_2, \ldots,$ and $x > x_{\mathrm{bp}}^{(N-1)}$ as $R_N$. For $N > 2$ during one drive cycle, a trajectory after the transient motion enters and leaves the regions $R_1$ and $R_N$ once, while twice the other regions. If we denote $T_{\mathrm{MR}}^{(i)}$ as the mean residence time in the $i$th region, then at $D = D_{\mathrm{MAX}}$ we realize that

$$T_{\mathrm{MR}}^{(1)} + 2\sum_{i=2}^{N-1} T_{\mathrm{MR}}^{(i)} + T_{\mathrm{MR}}^{(N)} = T. \tag{7}$$

For each fixed value of $N$, the mean residence times in each of the $N$ regions are all the same. Figure 6(a) displays the numerically computed $T_{\mathrm{MR}}$ at $D = D_{\mathrm{MAX}}$ as a function of $N$. We can clearly see the effect of $N$ on the mean residence time $T_{\mathrm{MR}}$ at

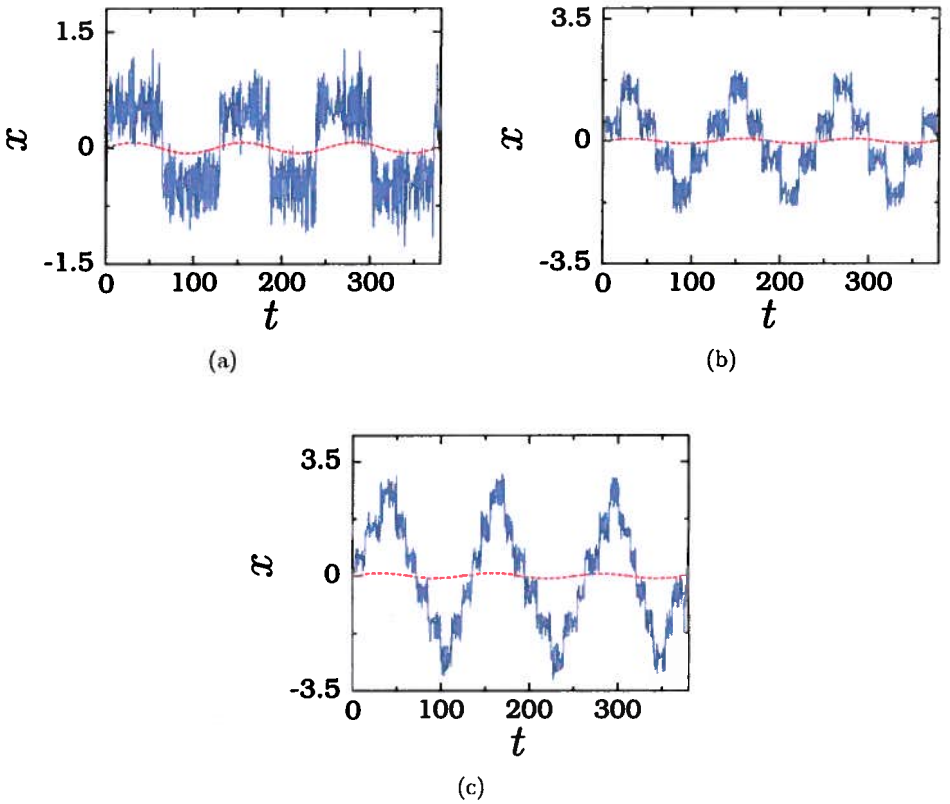


Fig. 5. $x(t)$ versus $t$ for three even integer values of $N$ at $D = D_{\mathrm{MAX}}$ at which SNR is maximum. Similar periodic switching to coexisting states occurs for $N = 3, 5, \ldots$. (a) $N = 2$, $D_{\mathrm{MAX}} = 0.14$, (b) $N = 4$, $D_{\mathrm{MAX}} = 0.172$ and (c) $N = 6$, $D_{\mathrm{MAX}} = 0.25$.

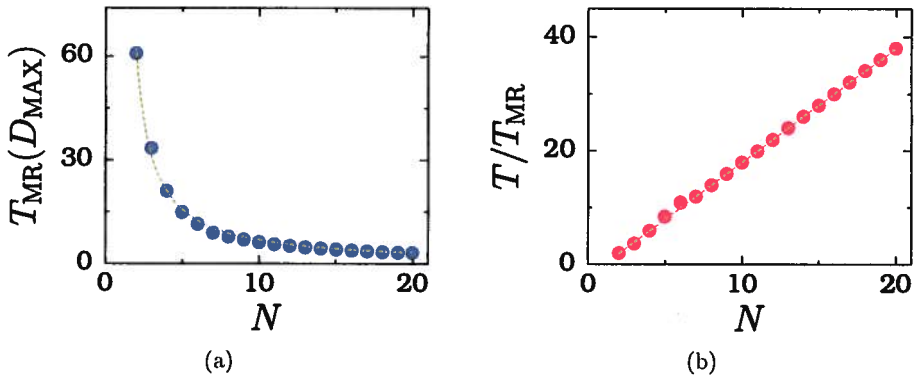


Fig. 6. (a) Dependence of mean residence time $T_{MR}$ of a trajectory about an equilibrium point on the total number of coexisting states $N$. Solid circles are the numerically computed values of $T_{MR}$. Continuous line represents the relation $T_{MR} = T/[2(N-1)]$ where $T = 2\pi/\omega$. (b) Plot of $T/T_{MR}$ versus $N$. Solid circles are the numerically computed data and the continuous line corresponds to $T/T_{MR} = 2(N-1)$.

resonance ($D = D_{MAX}$). It decreases with $N$ following the simple relation $T_{MR} = T/[2(N-1)]$ where $T = 2\pi/\omega$. This is clearly evident in Fig. 6(b) showing $T/T_{MR}$ (measuring the number of switches per drive cycle) versus $N$. The $x$-component values of the equilibrium points of the noise free and unforced system are equidistant and the function $F(x)$ has equidistant breakpoints and the barrier heights at the breakpoints are all the same. Due to these properties, the $T_{MR}$ of a trajectory in all the regions are the same. For $N = 2$ at $D = D_{MAX} = 0.14$ [see Fig. 5(a)] the mean residence time $T_{MR} = T/2$. While for $N = 4$, at $D = D_{MAX} = 0.172$ the corresponding $T_{MR}$ is $T/6$. For $N = 6$ we found $D = D_{MAX} = 0.25$ and $T_{MR} = T/10$.

For $D < D_c$ and for an initial condition, the long time motion (after leaving the motion corresponding to first 100 drive cycles of the external periodic force as a transient) is confined around any one of the equilibrium points. The equilibrium point about which motion occurs depends on the initial conditions. For both $D < D_c$ and $D \geq D_c$, the state variables $(x(t), y(t), z(t))$ depend on initial conditions. We computed SNR and $T_{MR}$ for several set of values of $D$ and initial conditions. The variation of SNR and $T_{MR}$ with initial conditions is found to be negligible. That is, the characteristic features of SR are insensitive to initial conditions.

## 3. Signal Detection Using Stochastic Resonance

Next, we discuss the problem whether it is possible to realize a mean residence time based signal detection making use of the modified Chua's circuit. Recently, residence time based detection strategies for nonlinear sensors have been suggested [Gammaitoni & Bulsara, 2002; Bulsara *et al.*, 2003; Dari *et al.*, 2010]. In this section, we use SR in system (1) for weak dc and ac signal detection by introducing an asymmetry in the characteristic function $F(x)$. Specifically, we consider the mean residence time asymmetry in the noisy multi-stable system.

By an additional dc signal we can alter the barrier height at one or more breakpoints. In the absence of a dc signal, distributions of residence times as well as mean residence times about various coexisting states are the same. They can be changed by an additional dc signal and the difference in the mean residence times can be used to measure the amplitude of the input dc signal.

Suppose we feed a dc signal, say $d$, to the modified Chua's circuit so that the functions $F_1(x)$ and $F_2(x)$ are modified into

$$F_1(x) \to F_1(x) - \xi A g, \tag{8a}$$

$$F_2(x) \to F_2(x) - \xi A g, \tag{8b}$$

where

$$g = \begin{cases} d, & \text{if } (x + 2jA) < 0 \text{ for } F_1(x) \\ d, & \text{if } (x + (2j+1)A) < 0 \text{ for } F_2(x) \\ 0, & \text{otherwise} \end{cases} \tag{8c}$$

and assume that $d > 0$. For simplicity we consider the system with only two breakpoints and three equilibrium points ($N = 3$) which can be realized for $F = F_2(x)$ with $n = 1$. Figure 7 shows the plot of $F_2(x)$ versus $x$ for $n = 1$, $d = 0$ and 1. We can clearly notice the influence of $d$. The barrier

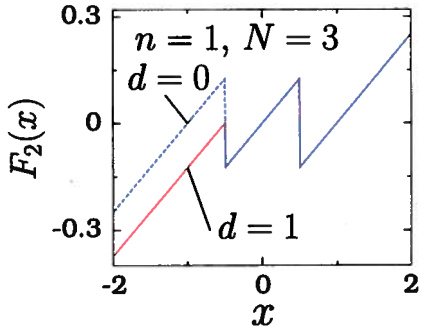


Fig. 7. Plot of $F_2(x)$ given by Eqs. (3) and (8) with $n = 1$ (that is, $N = 3$), $\xi = 0.25$, $A = 0.5$ and for $d = 0$ and 1.

heights at the breakpoints are the same for $d = 0$. When $d \neq 0$ the barrier height at $x_{\rm bp}^{(1)} = -0.5$ is less than that at $x_{\rm bp}^{(2)} = 0.5$. For arbitrary $N$ and $d \neq 0$ the heights of the barriers at $x_{\rm bp} < 0$ are altered by the input dc signal. In the absence of noise and in the presence of weak periodic force, the system has three orbits about the equilibrium points $x_{\rm e} = -1, 0, 1$. We call the orbits around the points $x_{\rm e} = -1, 0, 1$ as the left-, middle- and right-orbits respectively. When noise is introduced, SNR becomes maximum at an optimal noise intensity and the system displays SR.

In the presence of a dc signal the mean residence time of a trajectory on the left-orbit is different from that on, say, the right-orbit. We define $\Delta T_{\rm MR} = T_{\rm MR}^{\rm R} - T_{\rm MR}^{\rm L}$ where $T_{\rm MR}^{\rm R}$ and $T_{\rm MR}^{\rm L}$ are the mean residence times on the right- and the left-orbits, respectively. We calculate numerically $\Delta T_{\rm MR}$ for a range of values of $d$ for $D = 0.14$ and for a few fixed values of $N$. The result is presented in Fig. 8. Interestingly, $\Delta T_{\rm MR} = sd$. The values of

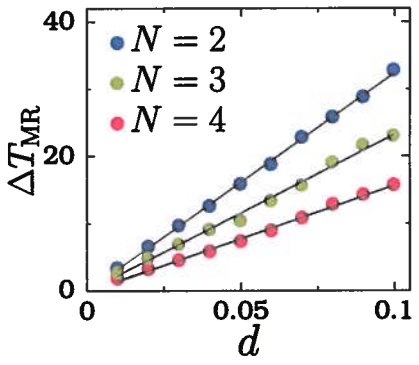


Fig. 8. Variation of $\Delta T_{\rm MR}$ with the dc signal $d$ for three fixed values of $N$ with $D = 0.14$. The symbols are numerical data while the continuous lines are the best straight-line fit.

$s$ for $N = 2$, 3 and 4 are 323.87, 232.62 and 158.13 respectively.

Ac signal detection is also possible using SR in the modified Chua's circuit. Suppose both frequency ($\omega$) and amplitude ($f$) of the input signal, for example $f \sin \omega t$, are unknown. When the intensity of the noise is varied, we notice that the peak in the power spectrum at the frequency (or its integral multiple) of the input periodic signal alone shows the signature of SR, that is, it increases, reaches a maximum at an optimum noise intensity and then decreases. This property can be used to identify the frequency $\omega$ of the input signal. For a fixed noise intensity, we can compute SNR and then making use of the predetermined relation between the amplitude $f$ and SNR we can determine the amplitude $f$ of the unknown input signal. It is noteworthy to point out that the relation between $f$ and SNR is found to be linear. Figure 9 shows $f$ and $\omega$ versus SNR. The dependence of SNR on $\omega$ is also linear.

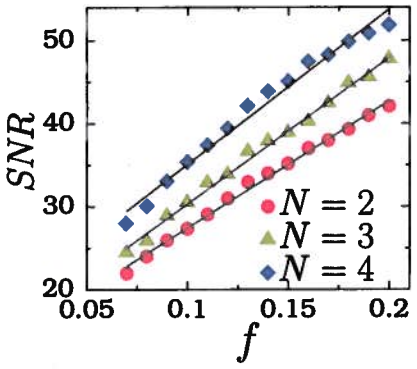


(a)

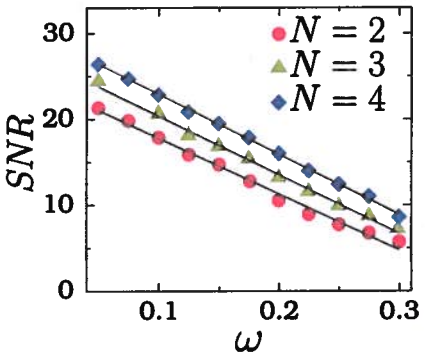


(b)

Fig. 9. Variation of SNR with (a) the amplitude $f$ and (b) the frequency $\omega$ of the input periodic signal for $N = 2$, 3, 4 and $D = 0.14$. In (a) $\omega = 0.05$ and in (b) $f = 0.07$. The symbols are numerical result and the continuous lines are the best straight-line fits.

## 4. Coherence Resonance

The modified Chua's circuit Eq. (1) exhibits CR in the absence of input periodic signal. The values of the parameters in Eq. (1) are the same as those used in SR analysis except $f = 0$. We analyze the response of the system by varying the noise intensity for various fixed values of $N$.

Prior to a detailed characterization of CR, we first show a signature of it in the power spectrum of the $x$-component of system (1). Figure 10 presents the power spectrum for three values of noise intensity for $N = 2$. Even though there is no input periodic signal of a definite frequency, the power spectrum shows a dominant peak at the particular frequency $\omega_0 \approx 0.045$. The presence of a dominant frequency in the trajectory of the system indicates the rotational motion about the equilibrium points. Additional peaks are not found for a wide range of noise intensity. The value of $\omega_0$ is found to be the same for other values of $N$. In Fig. 10 we notice that the width and the height of the peak in the power spectrum increase with increase in $D$ but in different rates.

The temporal order in the noise-induced dynamics is often quantified in terms of correlation time $\tau_c$ [Pikovsky & Kurths, 1997]. For the $x$-component of the state variable of the system, the normalized autocorrelation function is given by

$$C(\tau) = \frac{\langle \bar{x}(t)\bar{x}(t+\tau)\rangle}{\langle(\bar{x}(t))^2\rangle}, \tag{9}$$

where $\bar{x} = x - \langle x\rangle$. Then the correlation time $\tau_c$ is

$$\tau_c = \int_0^\infty C^2(\tau)d\tau. \tag{10}$$

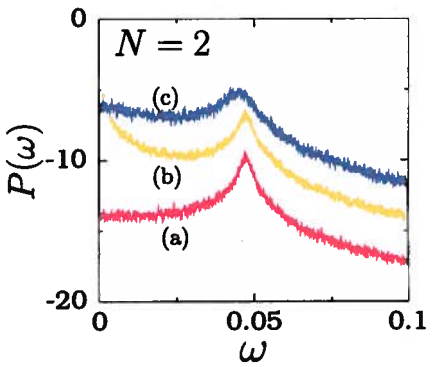


Fig. 10. Normalized power spectrum of $x$-component of the system (1) for three values of noise intensity in the absence of external periodic force. The values of $D$ for the spectra (a), (b) and (c) are 0.01, 0.058 (optimum value) and 0.1 respectively.

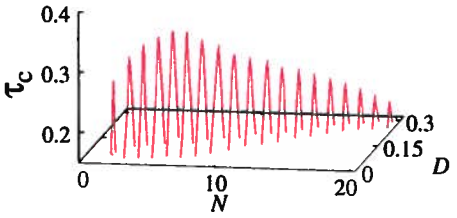


Fig. 11. Variation of correlation time with the noise intensity $D$ for various fixed values of $N$.

For a time series, the larger the value of $\tau_c$ the larger the temporal coherence. $C(\tau)$ is numerically computed for $0 < \tau < \tau'$ in steps of 0.01. For each $\tau$, after leaving a sufficient transient motion, $x(t)$, $t' < t < t' + 10^5$ is used for the computation of various average quantities in Eq. (9). $C(\tau)$ exhibits damped oscillation. $\tau'$ is chosen suitably so that for $\tau > \tau'$, $|C(\tau)| < 10^{-5}$.

Figure 11 shows $\tau_c$ versus the noise intensity $D$ for various fixed values of $N$. The $\tau_c$ versus $D$ profile resembles the SNR profile shown in Fig. 2 for SR. For each fixed value of $N$, $\tau_c$ increases with increasing $D$, reaches a maximum at an optimum noise intensity and then decreases. In Fig. 12(a) the value of $D_{MAX}$ at which $\tau_c$ becomes maximum increases with increasing $N$. In Fig. 12(b) the variation of maximum of $\tau_c$ with $N$ is similar to the variation of $SNR_{MAX}$ with $N$. $\tau_{c,MAX}$ is also found to be maximum for $N = 6$.

Another statistical measure of CR is the quantity $\beta_s$ given by [Sun *et al.*, 2008]

$$\beta_s = 10\log_{10}\left(\frac{H}{W}\right) \text{dB}, \tag{11}$$

where $H$ is the height of the peak in the power spectrum of the state variable, say, $x$ at the dominant frequency $\omega_0$ shown in Fig. 10. $W = \Delta\omega/\omega_0$ where $\Delta\omega$ is the half-width of the power spectrum about $\omega_0$. $\beta_s$ describes coherence in switching. $H$ and $W$ vary in different rates with $D$. The value of $D$ at which $\beta$ becomes maximum is considered as the optimum noise intensity $D_{MAX}$. Figure 13 shows the dependence of $\beta_s$ on $D$ for three values of $N$. For $N = 2$, 4 and 6, both $\beta_s$ and $\tau_c$ are maximum at $D = 0.06$, 0.08 and 0.09, respectively.

To gain more insight into the noise-induced CR dynamics, we consider the mean residence times about the coexisting states. For very small noise intensity, the motion is mostly confined to an equilibrium point and very rare switching between the coexisting states occurs. In SR, the noise-induced

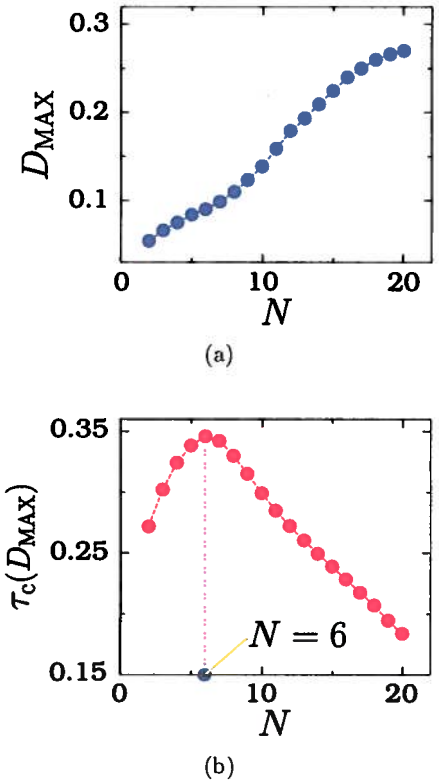


Fig. 12. Variation of (a) $D_{MAX}$, the value of $D$ at which correlation time becomes maximum and (b) $\tau_c$, computed at $D = D_{MAX}$, with the number of equilibrium points $N$.

switching is assisted by the periodic force. Consequently, resonance is realized when there is a synchronization between the switching motion and the input periodic signal. In the case of CR even though there is no input periodic signal, almost periodic switching between the coexisting states is found to occur at an optimum noise intensity. Figure 14 illustrates the nature of evolution of the $x$-component of the system at CR for three values of $N$. We

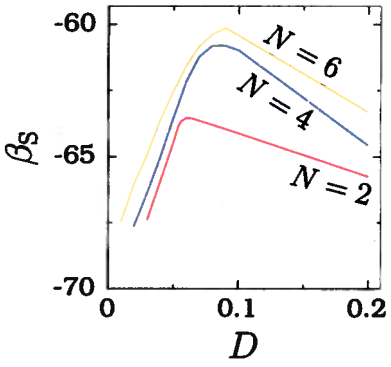


Fig. 13. CR parameter $\beta_s$ versus the noise intensity for three values of $N$.

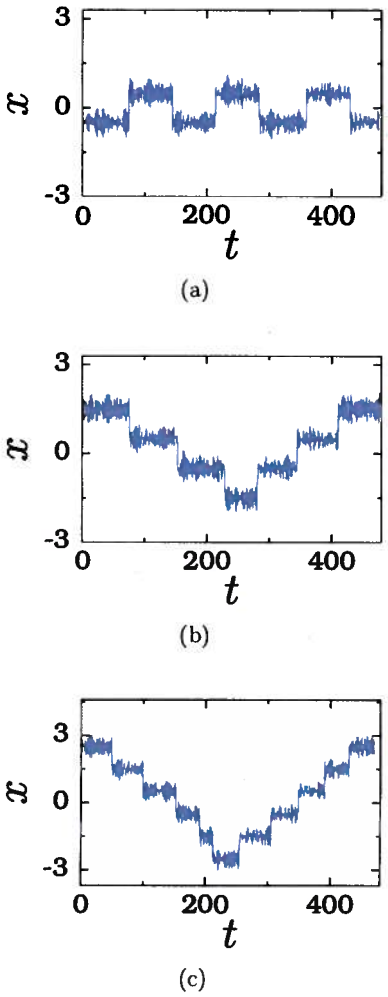


Fig. 14. The coherent switching dynamics at $D_{MAX}$ for three values of $N$. (a) $N = 2$, $D_{MAX} = 0.058$, (b) $N = 4$, $D_{MAX} = 0.08$ and (c) $N = 6$, $D_{MAX} = 0.09$.

can clearly see a staircase-like switching among the coexisting states.

Figure 15(a) shows the variation of mean residence time at resonance ($D = D_{MAX}$) with $N$. $T_{MR}$ decreases with increase in $N$. In Fig. 15(b) the quantity $T/T_{MR}$, where $T = 2\pi/\omega_0$, varies linearly with $N$. We find $T/T_{MR} = aN + b$ where $a = 0.37$ and $b = 1.2$, while for SR, $T/T_{MR} = 2(N - 1)$ with $T = 2\pi/\omega$. The features of CR are found to be insensitive to initial conditions.

CR is also useful for dc signal detection (addition of an unknown ac signal and noise leads to SR). We follow the same methodology considered in Sec. 3 in the case of SR. Figure 16 shows the numerically computed $\Delta T_{MR} = T^R_{MR} - T^L_{MR}$ as a function of the dc signal $d$ for $N = 2$, 3 and 4. For all the three values of $N$, the quantity $\Delta T_{MR}$ varies

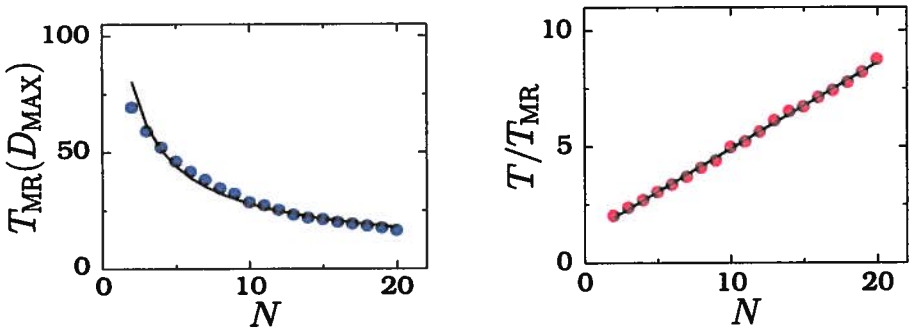


Fig. 15. (a) Plot of the mean residence time $T_{MR}$ at $D = D_{MAX}$ versus $N$ of system (1) driven by external noise in the absence of periodic input signal. (b) $T/T_{MR}$ versus $N$ where $T = 2\pi/\omega_0$, $\omega_0 = 0.045$.

linearly with $d$ as $\Delta T_{MR} = sd$. The value of $s$ for $N = 2$, 3 and 4 are calculated as 106, 87 and 69 respectively.

Few methods are available for signal detection. A straight-forward approach is the computation of Fourier transform of the time series of a given signal. It shows dominant peaks at the various frequencies present in the signal. In most of the sensors, occurrence of harmonics in the power spectrum is often used to detect the frequencies present in the signal. A feedback mechanism also exists for dc signal measurement. Some of the drawbacks of this scheme are given in [Bulsara *et al.*, 2003]. If the amplitude of the signal at a particular frequency is so weak then the Fourier transform technique may not be helpful. In this case, we can make use of SR, CR and vibrational resonance (VR) phenomena. In the VR approach, a nonlinear system is driven by a weak periodic force of frequency, say, $\omega$ and another periodic force of relatively high frequency $\Omega$ with $\Omega \gg \omega$. A difficulty with this method is that the frequency $\Omega$ of the second periodic force should be $\gg \omega$. In order to choose the value of $\Omega$ we need to know the range of the unknown frequency $\omega$. In this approach, a dc signal cannot be easily predictable.

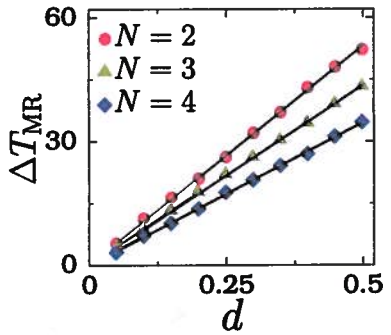


Fig. 16. Dependence of $\Delta T_{MR}$ on the applied input dc signal $d$ for three values of $N$ and $D = D_{MAX}(N)$.

Interestingly, in the modified Chua's circuit system, the height of the barrier at a breakpoint can be altered by the addition of a dc signal. This leads to asymmetry in the mean residence times of the trajectory about the stable equilibrium points when the system is subjected to noise. The asymmetry can be used to determine the presence of dc signal through both SR and CR. Also, we have pointed out the determination of unknown frequency and amplitude of a signal making use of SR in the system (1). The mean residence time based signal detection can be implemented experimentally [Bulsara *et al.*, 2003]. It is noteworthy to mention that as pointed out in [Nikitin *et al.*, 2003] the measurement error occurring due to the finite time interval of the signal is minimum at the resonance.

## 5. Conclusion

In conclusion the effects of multiple coexisting equilibrium points on both SR and CR are numerically investigated with reference to a modified Chua's circuit model equation. We mainly focused on the variation of statistical measures with the number of equilibrium points at the optimum noise intensity at which resonance occurs. The number of equilibrium points gives rise to similar effects for both resonances. Another notable result is that SR occurs, that is, SNR becomes maximum only when the mean residence times about the coexisting states are all same and equal to $T/[2(N-1)]$ where $T$ is the period of the input periodic signal. On the other hand, in the absence of an input periodic signal, CR takes place when the mean residence times about the coexisting states are same and equal to

$T_{MR}(D_{MAX}) = T/(aN + b)$ where $a = 0.37$ and $b = 1.2$ and $T = 2\pi/\omega_0$ with $\omega_0 = 0.045$. Furthermore, the variation of SNR (in the case of SR) and correlation time $\tau_c$ (in the case of CR) with number of equilibrium points is nonmonotonic and is maximum at $N = 6$. $T_{MR}$ and $D_{MAX}$ also depend on $N$. The two resonances reported in this paper can be realized experimentally in the modified Chua's circuit system with multiple equilibrium points and breakpoints and exploiting them for weak signal detection will have practical applications.

## References


Aziz-Alaoui, M. A. [1999] "Differential equations with multispiral attractors," *Int. J. Bifurcation and Chaos* **9**, 1009–1040.

Borromeo, M. & Marchesoni, F. [2006] "Vibrational ratchets," *Phys. Rev. E* **73**, 016142-1–8.

Borromeo, M. & Marchesoni, F. [2007] "Artificial sieves for quasimassless particles," *Phys. Rev. Lett.* **99**, 150605-1–4.

Boukabou, A., Sayoud, B., Boumaiza, H. & Mansouri, N. [2009] "Control of $n$-scroll Chua's circuit," *Int. J. Bifurcation and Chaos* **19**, 3813–3822.

Bulsara, A. R., Seberino, C., Gammaitoni, L., Karlsson, M. F., Lundqvist, B. & Robinson, J. W. C. [2003] "Signal detection via residence-time asymmetry in noisy bistable devices," *Phys. Rev. E* **67**, 016120-1–21.

Campos-Canton, E., Barajas-Ramirez, J. G., Solis-Perales, G. & Femat, R. [2010] "Multiscroll attractors by switching systems," *Chaos* **20**, 013116-1–6.

Dari, A., Bosi, L. & Gammaitoni, L. [2010] "Nonlinear sensors: An approach to the residence time detection strategy," *Phys. Rev. E* **81**, 011115-1–10.

Gammaitoni, L., Hänggi, P., Jung, P. & Marchesoni, F. [1998] "Stochastic resonance," *Rev. Mod. Phys.* **70**, 223–287.

Gammaitoni, L. & Bulsara, A. R. [2002] "Noise activated nonlinear dynamic sensors," *Phys. Rev. Lett.* **88**, 230601-1–4.

Han, F., Yu, X., Wang, Y., Feng, Y. & Chen, G. [2003] "$N$-scroll chaotic attractors by second-order system and double-hysteresis blocks," *IEEE Electron. Lett.* **39**, 1636–1637.

Jung, P. [1993] "Periodically driven stochastic systems," *Phys. Rep.* **234**, 175–295.

Kallunki, J., Dube, M. & Ala-Nissila, T. [1999] "Stochastic resonance and diffusion in periodic potentials," *J. Phys.: Condens. Matter* **11**, 9841–9850.

Kim, Y. W. & Sung, W. [1998] "Does stochastic resonance occur in periodic potentials?" *Phys. Rev. E* **57**, R6237–6240.

Landa, P. S. & McClintock, P. V. E. [2000] "Vibrational resonance," *J. Phys. A: Math. Gen.* **33**, L433–438.

Lu, J. & Chen, G. [2006] "Generating multiscroll chaotic attractors: Theories, methods and applications," *Int. J. Bifurcation and Chaos* **16**, 775–858.

McDonnell, M. D., Stocks, N. G., Pearce, C. E. M. & Abbott, D. [2008] *Stochastic Resonance* (Cambridge University Press, Cambridge).

Nicolis, C. [2010] "Stochastic resonance in multistable systems: The role of intermediate states," *Phys. Rev. E* **82**, 011139-1–9.

Nikitin, A., Stocks, N. G. & Bulsara, A. R. [2003] "Signal detection via residence times statistics: Noise-mediated minimization of the measurement error," *Phys. Rev. E* **68**, 036133-1–4.

Ozoguz, S., Elwakil, A. S. & Salama, K. N. [2002] "$n$-scroll chaos generator using a nonlinear transconductor," *IEEE Electron. Lett.* **38**, 685–686.

Pikovsky, A. S. & Kurths, J. [1997] "Coherence resonance in a noise-driven excitable system," *Phys. Rev. Lett.* **78**, 775–778.

Rajasekar, S., Abirami, K. & Sanjuan, M. A. F. [2011] "Novel vibrational resonance in multistable systems," *Chaos* **21**, 033106-1–7.

Saikia, S., Jayannavar, A. M. & Mahato, M. C. [2011] "Stochastic resonance in periodic potentials," *Phys. Rev. E* **83**, 061121-1–9.

Sun, X., Perc, M., Lu, Q. & Kurths, J. [2008] "Spatial coherence resonance on diffusive and small-world networks of Hodgkin–Huxley neurons," *Chaos* **18**, 023102-1–7.

Tang, K. S., Man, K. F. & Chen, G. [2001] "Digitized $n$-scroll attractor model for secure communications," *Proc. IEEE Int. Symp. Circ. Syst.*, Vol. 3, pp. 787–790.

Yalcin, M. E., Ozoguz, S., Suykens, J. A. K. & Vandewalle, J. [2001] "$n$-scroll chaos generators: A simple circuit model," *IEEE Electron. Lett.* **37**, 147–148.

Yalcin, M. E., Suykens, J. A. K. & Vandewalle, J. [2004a] "True random bit generation from a double scroll attractor," *IEEE Trans. Circuits Syst.-I* **51**, 1395–1404.

Yalcin, M. E., Suykens, J. A. K. & Vandewalle, J. [2004b] "A double scroll based true random bit generator," *Proc. IEEE Int. Symp. Circuits Systems*, pp. 581–584.

Yu, S. M., Lu, J., Leung, H. & Chen, G. [2005] "Design and implementation of $n$-scroll chaotic attractors from a general jerk circuit," *IEEE Trans. Circuits Syst.-I: Fundam. Th. Appl.* **52**, 1459–1476.

Yu, S., Tang, W. K. S. & Chen, G. [2007] "Generation of $n \times m$-scroll attractors under a Chua-circuit framework," *Int. J. Bifurcation and Chaos* **17**, 3951–3964.

Zhong, G. Q., Man, K. F. & Chen, G. [2002] "A systematic approach to generating $n$-scroll attractors," *Int. J. Bifurcation and Chaos* **12**, 2907–2916.